Submitted to *Journal of Vibration and Acoustics*, Feb. 2000
Approved for Unlimited Release, LA-UR-00-672

Vibration-Based Damage Identification in Structures Exhibiting Axial and Torsional Response

T. A. Duffey[1], S. W. Doebling[2], C. R. Farrar[3], W. E. Baker[4], W. H. Rhee[5]

Engineering Analysis Group
Engineering Sciences & Applications Division
Los Alamos National Laboratory
Los Alamos, NM, 87545

CORRESPONDING AUTHOR:

Scott W. Doebling
Los Alamos National Laboratory, M/S P946
Los Alamos, NM, 87545
Voice: (505) 667-6950 FAX: (505) 665-2137
doebling@lanl.gov

[1] Consulting Engineer, Member ASME
[2] Technical Staff Member, Member ASME
[3] Technical Staff Member, Materials Behavior Team Leader
[4] Consultant
[5] Graduate Research Assistant. Also: Ph. D. Candidate, Texas Tech University, Lubbock, Texas.

Abstract

A method is derived to detect and localize linear damage in a structure using the measured modal vibration parameters. This method is applicable when the vibration strain energy is stored in the axial or torsional modes, which differentiates it from previously derived strain-energy-based methods. The new method is compared to the previously derived flexibility-change method for comparison. Both methods are verified by application to an analytical eight degree of freedom model. Experimental validation for both methods is also presented by application to an experimental eight degree of freedom spring-mass structure.

1 Introduction

A wealth of algorithms exists for identifying the existence and location of damage in structural and mechanical systems, such as those reviewed by Doebling, et al. (1996, 1998). At the core, they all compare some features of the measured structural response to features of a previously measured structural response to assess whether damage has occurred. When the structure is assumed to behave linearly both before and after damage, the damage identification technique is known as a "linear method." One of the more commonly used linear methods for vibration-based damage identification is the so-called "damage index" or "strain energy" method originally presented by Stubbs, et al. (1992). This method uses a ratio of strain energy in discrete structural elements before and after damage as the feature to compare using the damage identification scheme. Often this method is applied to structures where it is assumed that the structures are dominated by flexural vibrations.(e.g. Farrar and Jauregui, 1996)). However, there are many situations where the structure responds in an axial or torsional fashion. In these cases, the assumption of flexural behavior is not valid and so the damage index method cannot be applied as originally developed. The purpose of this paper is to derive an extension to the damage index method that is applicable to structures undergoing vibrations predominantly in axial or torsional modes.

The structural health-monitoring problem is best viewed in the context of a statistical pattern recognition paradigm. This paradigm can be described as a four-part process: 1.) operational evaluation, 2.) data acquisition & cleansing, 3.) feature extraction & data reduction, and 4.) statistical model development. Operational evaluation answers four questions regarding the implementation of a structural health monitoring system: 1. How is damage defined for the

system being monitored? 2. What are the conditions, both operational and environmental, under which the system to be monitored functions? 3. What are the limitations on acquiring data in the operational environment?, and 4. What are the economic and/or life safety motives for performing the monitoring? Operational evaluation begins to define why the monitoring is to be done and begins to tailor the monitoring to unique aspects of the system and unique features of the damage that is to be detected.

The data acquisition portion of the structural health monitoring process involves selecting the types of sensors to be used, the locations where the sensors should be placed, the number of sensors to be used, and the data acquisition/storage/transmittal hardware. Other considerations that must be addressed include how often the data should be collected, how to normalize the data, and how to quantify the variability in the measurement process. Data cleansing is the process of selectively choosing data to accept for, or reject from, the feature selection process. Filtering and data decimation are two of the most common methods for data cleansing.

The area of the structural health monitoring that receives the most attention in the technical literature is feature extraction. Feature extraction is the process of the identifying damage-sensitive properties, derived from the measured vibration response, which allow one to distinguish between the undamaged and damaged structure. Almost all feature extraction procedures inherently perform some form of data compression. Data compression into feature vectors of small dimension is necessary if accurate estimates of the feature statistical distribution are to be obtained.

Statistical model development is concerned with the implementation of the algorithms that analyze the distribution of extracted features in an effort to determine the damaged state of the structure. The algorithms used in statistical model development fall into the three general categories: 1. Group Classification, 2. Regression Analysis, and 3. Outlier Detection. The appropriate algorithm to use will depend on the ability to perform *supervised* or *unsupervised* learning. Supervised learning refers to the case were examples of data from damaged and undamaged structures are available. Unsupervised learning refers to the case were data is only available from the undamaged structure.

The focus of this paper is on feature extraction for structure exhibiting axial or torsional response when subjected to dynamic excitation. The features of interest in this case are the changes in strain energy in discrete elements of the structure between the undamaged and damaged states. The method is compared to the “flexibility-change” method

presented by Pandey and Biswas (1994) for assessment. The flexibility-change method uses changes in the entries of the measured structural flexibility matrix as damage identification features. Both methods are applied to an analytical 8-DOF linear spring-mass system, which is a generalization of a multi-degree-of-freedom axial structure, for verification. (It should be noted that other studies on the same structure have been presented by Hemez and Doebling (1999).) Next, the methods are applied to experimental damage identification results obtained on an 8-DOF spring-mass system. The goal of the work is to detect the existence of damage (as indicated by reduction in stiffness of one or more of the elements) as well as to localize the damaged element(s). Further issues that are explored in this paper include the selection of the subset of modes to include in the analysis and the influence of multiple damage locations on the accuracy of the damage identification.

2 Theoretical Development

2.1 Damage Index Method for Axial and Torsional Structures

The damage index method, developed by Stubbs, et al. (1992) locates damage in structures undergoing flexural vibration given their characteristic mode shapes measured before and after damage. For structures undergoing bending, it has been demonstrated in many cases that only a few modes are required to obtain reliable results. The method is based on a comparison of the modal strain energies in undamaged and damaged beams. It is straightforward to re-derive the method to account for axial, as opposed to bending, vibrations. The bending strain energy for a Bernoulli-Euler beam is

$$U = \frac{1}{2} \int_0^{\ell} EI \left(\frac{d^2 w}{dx^2} \right)^2 dx \tag{1}$$

where *EI* is flexural rigidity, ℓ denotes beam length, $w(x)$ is transverse displacement, and *x* is the coordinate along the span of the beam. The corresponding energy expression for axial vibrations can be written

$$U = \frac{1}{2} \int_0^{\ell} AE \left(\frac{du}{dx} \right)^2 dx \tag{2}$$

where $u(x)$ denotes the in-plane (axial) displacement field, and AE denotes the axial rigidity.

Following the derivation of the Damage Index method for beam bending presented by Stubbs, et al. (1992) it is readily shown that the change in axial rigidity (as opposed to bending rigidity) at the k^{th} location in the structure for the i^{th} mode is given by

$$\frac{g_{ik}^{*}}{g_{ik}} = \frac{\int_{a_k}^{a_k+1}\left(\frac{d\psi_i^{*}}{dx}\right)^2 dx \Big/ \int_0^{\ell}\left(\frac{d\psi_i^{*}}{dx}\right)^2 dx}{\int_{a_k}^{a_k+1}\left(\frac{d\psi_i}{dx}\right)^2 dx \Big/ \int_0^{\ell}\left(\frac{d\psi_i}{dx}\right)^2 dx} \tag{3}$$

where ψ_i denotes the i^{th} normal mode shape and ( )* denotes the parameters of the damaged structure. The above expression is an index of the change in axial rigidity from the undamaged structure to the damaged structure where $a_k \le x \le a_{k+1}$ denotes the interval of the k^{th} region along the span of length ℓ. Because the mode shapes appear on both the top and the bottom, mass-normalized mode shapes are not required. Thus a measurement of the input excitation is not required, which greatly relaxes the constraints on the design of the vibration experiment. If the above equation is reapplied for each sub-region (i.e., element) along the span, a measure of axial rigidity change along the span for the i^{th} normal mode is produced. In order to use all measured modes, *n*, the damage index, α_k, for the k^{th} sub-region is defined as

$$\alpha_k = \frac{\sum_{i=1}^{n} g_{ik}^{*}}{\sum_{i=1}^{n} g_{ik}} \tag{4}$$

It should be noted that because the basic quantities of interest in calculating the damage index are the mode shapes, any damage occurring at a modal node (spatial location of near-zero response) of the modes included in Eq. (4) will not affect the mode shape and thus will not be detected.

An analogous damage index can be derived for the case of torsional vibration by using the torsional mode shapes θ_i. The strain energy for a member undergoing torsional motion is

$$U = \frac{1}{2} \int_0^{\ell} GJ \left(\frac{d\theta}{dx} \right)^2 dx \tag{5}$$

where $\theta(x)$ denotes the torsional displacement field, and GJ denotes the torsional rigidity. Then the torsional counterpart to Eq. (3) can be written as

$$\frac{g_{ik}^*}{g_{ik}} = \frac{\int_{a_k}^{a_k+1} \left(\frac{d\,\theta_i^*}{dx} \right)^2 dx \Big/ \int_0^{\ell} \left(\frac{d\theta_i^*}{dx} \right)^2 dx}{\int_{a_k}^{a_k+1} \left(\frac{d\,\theta_i}{dx} \right)^2 dx \Big/ \int_0^{\ell} \left(\frac{d\,\theta_i}{dx} \right)^2 dx} \tag{6}$$

2.2 Flexibility Change Method for Axial and Torsional Structures

The flexibility change method is based upon differences in the flexibility of the structure before and after damage has occurred. For the flexural vibrations of beams, Pandey and Biswas (1994) show that damage could both be detected and located from just the first two (or three) measured modes of the structure. The method differs somewhat from the more familiar methods of damage detection based on changes in the modal parameters of a system (i.e., resonant frequencies, mode shapes, and modal damping). The authors are unaware of any application of the method to problems involving axial loading. The flexibility change method is applied to the 8-DOF spring-mass model in this paper and found to be particularly robust in both the detection of the presence of damage as well as the location of the damage. The location of damage is directly indicated by a step change in a flexibility indicator at the point of damage. Further, the *magnitude* of this indicator does not depend upon damage location, in contrast to earlier work on beams reported by Pandey and Biswas. Because in real applications there is the distinct possibility of damage at more than one of the elements, the case of simultaneous damage at more than one element location was investigated as well. The flexibility change method was found to isolate two separate damage locations effectively.

As explained by Pandey and Biswas (1994) and Farrar and Jauregui (1996), the flexibility change method consists of the following: For the undamaged structure, the flexibility matrix, $[F]$, is formed from the modal data as:

$$[F] = [\Phi][\Omega]^{-1}[\Phi]^T \approx \sum_{i=1}^{n} \frac{1}{(\omega_i)^2} \{\phi_i\}\{\phi_i\}^T \tag{7}$$

where $\{\phi_i\}$ is the i^{th} mass-normalized mode shape, $[\Phi] = [\phi_1, \phi_2, ..., \phi_n]$ is the matrix of mass-normalized mode shapes, and ω_i is the i^{th} modal frequency. The modal stiffness matrix is $[\Omega] = diag(\omega_i^2)$ and n is the number of measured or calculated modes. The approximation in Eq. (7) comes from the fact that typically the number of modes identified is less than the number of degrees of freedom needed to accurately represent the motion of the structure.

Similarly, for the damaged structure,

$$[F^*] = [\Phi^*][\Omega^*]^{-1}[\Phi^*]^T \approx \sum_{i=1}^{n} \frac{1}{(\omega_i^*)^2} \{\phi_i^*\}\{\phi_i^*\}^T \tag{8}$$

where the asterisks signify properties of the damaged structure. From the pre- and post- damage flexibility matrices, a measure of the flexibility change caused by the damage can be obtained from the difference of the respective matrices, i.e.,

$$[\Delta F] = [F] - [F^*] \tag{9}$$

where $[\Delta F]$ represents the flexibility-change matrix. Now, for each column of matrix $[\Delta F]$ let $\bar{\delta}_j$ be the absolute maximum value of the element in the j^{th} column. Hence,

$$\bar{\delta}_j = \max|\delta_{ij}|, \; i = 1, ..., n \tag{10}$$

where $\bar{\delta}_{ij}$ are elements of matrix $[\Delta F]$. Then $\bar{\delta}_j$ is taken to be a measure of the flexibility change at each measurement location. The column of the flexibility matrix corresponding to the largest $\bar{\delta}_j$ indicates the degree of

freedom where damage is located. Other methods have been developed to evaluate damage using the measured flexibility matrix, and are reviewed by Doebling, et al. (1998).

3 Numerical Examples

Consider the linear 8-DOF spring-mass system shown in Figure 1**,** for which the free vibration response is described by solution of the generalized eigenvalue problem,

$$[K]\{\psi_i\} = \lambda_i [M]\{\psi_i\} \tag{11}$$

where $\lambda_i = \omega_i^2$. Here $[M]$ denotes the diagonal mass matrix, $[K]$ is the (symmetric) stiffness matrix, λ_i is the i^{th} eigenvalue (square of the i^{th} natural frequency) and $\{\psi_i\}$ denotes the i^{th} eigenvector (i^{th} mode shape). If $[M]$ is the identity matrix, Eq. (11) reverts to the standard eigenvalue equation as described by Feng and Owen (1996).

By inspection of Figure 1, the mass matrix is

$$[M] = \begin{bmatrix} m_1 & & & & & & & 0 \\ & m_2 & & & & & & \\ & & \cdot & & & & & \\ & & & \cdot & & & & \\ & & & & \cdot & & & \\ & & & & & \cdot & & \\ 0 & & & & & & & m_8 \end{bmatrix} \tag{12}$$

The stiffness matrix, [K], can readily be written as the following banded 8 x 8 symmetric matrix:

$$[K] = \begin{bmatrix} (k_1+k_2) & -k_2 & 0 & 0 & 0 & 0 & 0 & 0 \\ -k_2 & (k_2+k_3) & -k_3 & 0 & 0 & 0 & 0 & 0 \\ 0 & -k_3 & (k_3+k_4) & -k_4 & 0 & 0 & 0 & 0 \\ 0 & 0 & -k_4 & (k_4+k_5) & -k_5 & 0 & 0 & 0 \\ 0 & 0 & 0 & -k_5 & (k_5+k_6) & -k_6 & 0 & 0 \\ 0 & 0 & 0 & 0 & -k_6 & (k_6+k_7) & -k_7 & 0 \\ 0 & 0 & 0 & 0 & 0 & -k_7 & (k_7+k_8) & -k_8 \\ 0 & 0 & 0 & 0 & 0 & 0 & -k_8 & k_8 \end{bmatrix} \tag{13}$$

For illustrative purposes, consider a baseline 8-DOF system of unit masses and stiffnesses:

$$\begin{aligned} m_i &= 1 \text{ for } i = 1,8 \\ k_i &= 1 \text{ for } i = 1,8 \end{aligned} \tag{14}$$

The eight eigenvectors and corresponding eigenvalues for the generalized eigenvalue problem are readily determined numerically. According to Blevins (1984), the modal frequencies can be written as:

$$f_i = \frac{1}{\pi} sin\left[\frac{(2i\text{-}1)}{34}\pi\right], i = 1, 2, ..., 8 \tag{15}$$

Eight separate damage cases are considered: Each stiffness value is individually reduced 10-percent to a value of 0.9. A plot of natural frequency as a function of mode number for the baseline system and the eight perturbed systems is shown in Figure 2. Clearly, identification of damage by changes in natural frequency is not feasible, as a 10-percent stiffness change at only one location results in almost negligible natural frequency changes for the normal modes.

The effects of stiffness perturbations on mode shape changes are illustrated in Figure 3 and Figure 4. Figure 3 shows the normalized modal displacement of the first mode for the baseline unperturbed case as well as the eight perturbed (10-percent reduced stiffness) cases. Figure 4 is the corresponding set of plots for mode 8. Generally, it was found that the four highest modes do seem somewhat more sensitive to stiffness perturbations. In some cases, the percentage change can be quite substantial for individual degrees of freedom. Unfortunately, mode shapes are more

difficult to accurately obtain than frequencies, as shown for a particular case study by Doebling, et al. (1997). Moreover, no information can be gleaned from these natural frequency or modal shape changes regarding the location of the damage. However, it is possible that the damage index indicator and the flexibility change may provide better localization of the damage location than just the mode shapes and modal frequencies.

3.1 Application of the Damage Index Method

The damage index method was applied to the analytical 8DOF system, producing a set of α_k values from Eq. (4). Results are shown in Figure 5 for the case in which damage of 10% stiffness reduction was introduced in the third element. The location of damage at element 3 is readily apparent in Figure 5. It is important to note that Figure 5 is constructed utilizing the complete set of all eight (damaged and undamaged) modes.

3.2 Application of the Flexibility-Change Method

To implement the flexibility-change method, each mode shape of the baseline (undamaged) case is first mass-normalized as described by Thomson (1981). (Experimentally, this would be accomplished by making a driving point response measurement.) The generalized masses for each mode are calculated by forming the matrix product $[\Psi]^T [M][\Psi]$ where $[M]$ is the original mass matrix and $[\Psi]$ denotes the (unweighted) modal matrix. The diagonal terms of the matrix product denote the generalized mass, M_i. Then each of the columns of the modal matrix $[\Psi]$ is divided by the square root of the corresponding generalized mass term, M_i, resulting in the mass-normalized modal matrix $[\Phi]$.

Next, the flexibility of each of the 8 perturbed systems (stiffness reductions of 10-percent each) is calculated using Eq. (7). Then the difference between the original and the perturbed flexibility matrices are calculated using Eq. (9), and $\overline{\delta}_j$ is determined using Eq. (10). Normalized results are presented in Figure 6 for 10-percent damage in the first, second and third elements respectively. It is apparent that the detection of damage location is indeed possible for axial-loading applications and takes on a somewhat different form than for the beam bending examples discussed by Pandey and Biswas (1994). For the situation in Figure 6, damage is present in the element for which nonzero

differences in flexibility first appear. An advantage of this method, when applied to this axially loaded example, is that the location of damage is directly indicated by a step change at the point of damage. The method does, however, require mass-normalized mode shapes.

3.3 Damage at Multiple Locations

The next issue is that of damage at multiple locations. The flexibility-change results for the case of damage at DOF 3 and DOF 6 (a 10-percent reduction in stiffness at each location) is shown in Figure 7. Again, the method isolates both the presence and location of damage. Additional damage locations are indicated by subsequent step changes in the damage indicator.

3.4 Influence of Number of Modes Used

For axial (or torsional) problems, the influence of the number of lower modes utilized on the flexibility-change results is illustrated in Figure 8 for the case of 10-percent reduction in stiffness of k_4. In Figure 8, it is seen that the presence and location of damage is readily estimated using only the first mode for determining the change in flexibility. This observation is important because in practice, only a partial set of the lower modes is typically available. Further, for the particular 8-DOF example evaluated, a reasonable estimate of the magnitude of the damage indicator was provided using the first vibration mode only. Inclusion of the first three modes was sufficient to estimate the damage indicator (flexibility change) within a few percent.

4 Experimental Validation

Now that the implementation of the methods has been verified on an analytical simulation, the methods are applied to data from an experimental apparatus to validate the methods as legitimate techniques for identifying structural damage. The experimental apparatus is an 8 DOF spring-mass system. Linear damage was introduced at a variety of locations in the system and with a variety of magnitudes by replacing selected springs with less stiff counterparts.

The 8DOF system is formed with eight translating masses connected by springs, shown by schematic in Figure 9 and by photograph in Figure 10. Each mass is a disc of aluminum 25.4 mm thick and 76.2 mm in diameter with a

center hole. The hole is lined with a Teflon bushing. There are small steel collars on each end of the discs. The masses all slide on a highly polished steel rod that supports the masses and constrains them to translate along the rod. The masses are fastened together with coil springs epoxied to the collars that are, in turn, bolted to the masses as shown.

The undamaged configuration of the system is the state for which all springs are identical and have a linear spring constant. Linear damage in the model is simulated by replacing an original spring with another linear spring which has a spring constant less than that of the original. The replacement spring may be located between any pair of adjacent masses, and thus simulate different locations of damage. The replacement spring may have different degrees of stiffness reduction to simulate different levels of damage. The nominal values of the system parameters are as follows:

- **Mass 1**: 559.3 grams (This mass is located at the end where the shaker is attached or impact-hammer excitation is applied. It is greater than the others because of the hardware required to attach the shaker.)
- **Masses 2 through 8:** 419.4 grams
- Spring constants:
  - 56.7 kN/m (322 lb/in) (undamaged)
  - 52.6 kN/m (299 lb/in) (7% stiffness reduction)
  - 49.0 kN/m (278 lb/in) (14% stiffness reduction)
  - 43.0 kN/m (244 lb/in) (24% stiffness reduction)

Spring locations are designated sequentially, with the spring closest to the end of the system where the excitation is applied designated as #1, as shown in Figure 9. The level of stiffness reduction and the location of the reduced-stiffness spring describe the damage cases. Energy loss in the system is caused primarily by Coulomb friction. A common commercial silicon lubricant is applied between the Teflon bushings and the support rod. to minimize this friction. During these tests it was observed that the excitation force, whether from impulse or random excitation,

must be great enough to override the frictional effects. Each time that the system is disassembled to change a spring, careful alignment of the springs and masses is performed.

The data acquisition equipment used in this study was a Hewlett-Packard 3566A system. This system is composed of a model 35650 mainframe, 35653A source module, and five 35653A eight-channel input modules (which provided power for the accelerometers and performed the analog-to-digital conversion of the transducer signals). A 35651C signal-processing module performs the necessary FFT calculations. A laptop computer was used for data storage and as the platform for the software for controlling the data acquisition system. The force transducer used was a PCB type 204 (nominal sensitivity of 22.5 mv/N), and the accelerometers were Endevco type 2251 A-10 (nominal sensitivity of 10 mv/G). One accelerometer was located on each mass, for a total of eight measured acceleration DOF. The Rational Polynomial algorithm (Richardson and Formenti, 1982) was used to determine the required modal properties for each of the configurations tested by fitting a parametric form of the FRF to the measured FRF data. Tests performed included the baseline ("undamaged") configuration of the 8-DOF system as well as three levels of damage (7-14-, and 24-percent) sequentially applied at three different locations (springs 1, 5, and 7). Both impact-hammer excitation and random excitation tests were sequentially performed. All data used to generate the results presented herein along with further details of the experiments are available at

http://www.lanl.gov/projects/damage_id/.

4.1 Application of the Damage Index Method

Three levels of damage (7-, 14-, and 24-percent stiffness reduction) at three locations (spring 1, spring 5, and spring 7) were sequentially evaluated using the modified damage-index method. As an illustration, results for 24-percent damage at locations 1, 5, and 7 are shown in Figure 11, Figure 12, and Figure 13, respectively, for impact-hammer excitation. The results of the damage indicator for the first mode, first two modes, first three modes, and first four modes are shown in each case. The following observations can be made for the modified damage-index method at this significant level of damage:

- Damage at the extreme ends of the 8-DOF system (springs 1 and 7) is more readily identified than at an internal location (spring 5).

- Damage is readily detected using the first mode only. Inclusion of higher modes does not necessarily improve the identification of damage location.

Review of lower (7-percent, 14-percent) levels of damage indicated the following:

- Damage even at the 7-percent level could readily be detected (e.g., see Figure 14 for 7-percent stiffness reduction of spring 1).

- Damage at the intermediate (14-percent) level (not shown) was more difficult to detect than damage at lower and higher levels, i.e., the method readily determines the location of damage but does not provide a direct measure of the level of damage. This anomaly may have been due to friction induced by variations in alignment of the masses during the spring replacement process. This phenomenon was not observed in the simulated damage results, where higher levels of damage always resulted in more significant indications.

The modified damage-index method was also applied to random vibration data with similar results.

4.2 Application of the Flexibility-Change Method

The method was evaluated using the same data as for the modified damage-index method (7-, 14-, and 24-percent stiffness reduction at three locations (springs 1, 5, and 7). The following general observations were made:

- Surprisingly, detection of damage was actually best overall for the case of 7-percent damage, in contrast to results using the modified damage-index method. Again, variations in alignment of the masses during the spring replacement may have been a factor.

- Detection of damage was best at the extreme locations (Springs 1 and 7). Damage could only be detected at location 5 for the 7-percent damage level.

- The ability to detect damage improved as the number of included modes increased, as the flexibility matrix is better approximated with increased numbers of included modes. Recall that for the modified damage index method, best results were generally obtained using the first mode only.

Results for 7-percent damage are shown in Figure 15 and Figure 16 for damage at locations 1 and 5, respectively. In each of the figures, the four bars at each spring location denote, respectively, inclusion of the first mode only, modes 1 and 2, modes 1-3, and modes 1-4. In this case, damage is clearly indicated for 7-percent damage in spring 1 (Figure 15) as long as more than one mode is included. For 7-percent damage at spring 5 (Figure 16) damage is indicated in spring 5, but there appear to be false-positive damage indications at springs 2 and 3.

5 Conclusion

Two recently reported linear structural damage identification methods, previously developed for structures undergoing flexural vibrations, were applied to both simulated and experimental spring-mass systems undergoing axial response. These two methods are the "flexibility-change" method, which requires mass-normalized mode shapes and modal frequencies, and a modified form of the "damage index" method, which requires only arbitrarily normalized mode shapes. Both the flexibility-change method and the modified form of the damage index method were successful in detecting damage and in locating damaged elements for 10-percent reductions in element stiffnesses in a simulated spring-mass system.

For the experimental damage cases, the modified damage-index method performed well in locating damage at all three levels of damage investigated. The method, however, performed better at isolating damage at (exterior) spring locations 1 and 7 than for the interior spring location 5. Damage was successfully located using the first mode only. It was observed that the system seems to have significant off-axis motion at the interior DOF, and this factor is a possible reason why damage at the end points is more clearly identified. Results were not as favorable with the flexibility-change method. Although damage location could be detected for 7-percent damage at each location, results surprisingly deteriorated at 14-percent damage. It is speculated that increased variability in the experimental hardware possibly resulting from lack of repeatability in the assembly procedure is responsible for the deteriorated results at 14-percent damage. At the 24-percent level, damage could easily be located at spring locations 1 and 7, but not at location 5. Overall, results using this method were somewhat unreliable, depending strongly upon damage location, damage level, and number of modes included. The effects of experimental variability on the damage identification results were not considered in this research, and neither were the effects of nonlinear and frictional mechanics. It is speculated that the variability in these experiments was significant and these issues will be address

in future work. This issue highlights the need for statistical techniques that can account for measurement uncertainty and system variability in the damage identification process. Also, it is unrealistic to expect an acceleration measurement on each DOF of interest in a real application, so the effects of reduced sensor sets should be studied.

To date, the applications of vibration-based damage identification methods have been primarily focused on relatively simple structures such as beams and plates. By developing a library of "damage elements," the authors believe that it may be possible to construct a methodology of vibration-based damage identification, analogous to finite element discretization, which can be more readily applied to general structural and mechanical systems. The damage index method is particularly well suited for such development. The development of an axial or torsional element presented in this research provides the foundation for one element of such a code. Previous work of Stubbs, et al. (1992) and Cornwell, et al. (1999) provides the development of two additional elements (beams and plates) for such a code. Further development will be required for shell and continuum damage elements. Consideration of the fact that the vibration responses associated with internal degrees of freedom (those nodes not accessible to sensors mounted on the surface of the structure) are extremely difficult to measure must be addressed in the development of such a general purpose code. Also, difficulties associated with measuring rotational degrees of freedom will have to be addressed.

Future work (in progress) involves detection of nonlinear damage. The above-described 8-DOF system has been modified to simulate nonlinear damage by placing rods (impactors) on one mass that limit the amount of motion that the mass may move relative to an adjacent mass. Changing the amount of relative motion permitted before contact controls the magnitude of the nonlinearity. Methods of statistical pattern recognition (not dependent on modal analysis) are being applied to identify the presence of this nonlinear damage.

6 Acknowledgments

The authors would like to thank Prof. T. Burton, Texas Tech University, for helpful suggestions on this work. This work was performed under the auspices of the U. S. Department of Energy. Duffey, et al. (1998, 1999), first presented these results.

7 References

Blevins, R. D., 1984, *Formulas for Natural Frequency and Mode Shape* Krieger Publishing Company.

Cornwell, P.J., Doebling, S.W., and Farrar, C.R., 1999, "Application of the Strain Energy Damage Detection Method to Plate-Like Structures," *Journal of Sound and Vibration*, Vol. 224, No. 2, 359-374.

Doebling, S. W., Farrar, C. R., Prime, M. B. and Shevitz, D. W., 1996, "Damage Identification and Health Monitoring of Structural and Mechanical Systems from Changes in Their Vibration Characteristics: A Literature Review," Los Alamos National Laboratory Report LA-13070-MS.

Doebling, S. W., Farrar, C.R., and Goodman, R. S., 1997, "Effects of Measurement Statistics on the Detection of Damage in the Alamosa Canyon Bridge," *Proc. of the 15th International Modal Analysis Conference*, Orlando, FL, pp. 919-929.

Doebling, S. W., Farrar, C. R., and Prime, M. B., 1998, "A Summary Review of Vibration-Based Damage Identification Methods," *The Shock and Vibration Digest*, Vol. 30, No. 2, pp. 91-105.

Duffey, T. A., Farrar, C. R., and Doebling, S. W., 1998, "Damage Detection for Applications Undergoing Axial (Membrane) Response," in *Proceedings of the 16th International Modal Analysis Conference*, pp. 1278-1284.

Duffey, T. A., Baker, W. E., Farrar, C. R., and Rhee, W.H., 1999, "Detection of Damage in Axial (Membrane) Systems," in *Proceedings Of the 17th International Modal Analysis Conference*, pp. 876-881.

Farrar, C. R.and Jauregui, D. V., 1996, "Damage Detection Algorithms Applied to Experimental and Numerical Modal Data from the I-40 Bridge," Los Alamos National Laboratory Report LA-13074-MS.

Feng, Y. T. And Owen, D. R. J., 1996, "Conjugate Gradient Methods for Solving the Smallest Eigenpair of Large Symmetric Eigenvalue Problems," *International Journal for Numerical Methods in Engineering*, Vol. 39, pp 2209-2229.

Hemez, F.M. and Doebling, S.W., 1999, "Test-Analysis Correlation and Finite Element Model Updating for Nonlinear, Transient Dynamics," Proc. of the 17th International Modal Analysis Conference, Kissimmee, FL, Feb.1999, pp. 1501-1510.

Pandey, A. K. and Biswas, M., 1994, "Damage Detection in Structures Using Changes in Flexibility," *Journal of Sound and Vibration*, Vol. 169, No. 1, pp 3-17.

Richardson, M. H., and Formenti, D. L., 1982, "Parameter Estimation from Frequency Response Measurements using Rational Fraction Polynomials," *Proceedings of the 1st International Modal Analysis Conference*, Orlando, FL (Bethel, Conn., USA: Society for Experimental Mechanics.), pp. 167–181.

Stubbs, N., Kim, J.-T., and Topole, K., 1992, "An Efficient and Robust Algorithm for Damage Localization in Offshore Platforms," in *Proceedings of the ASCE Tenth Structures Congress*, pp. 543-546.

Thomson, W. T., 1981, *Theory of Vibration with Applications*, Prentice - Hall, Inc.

8 Figures & Tables

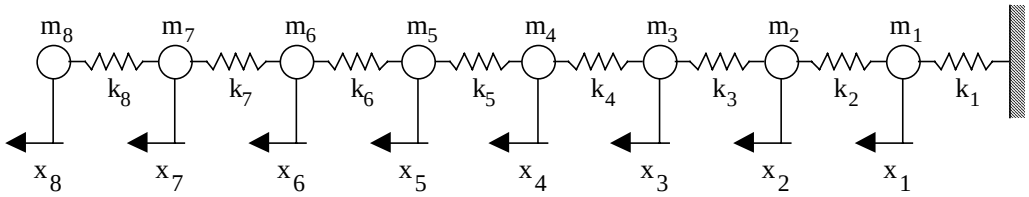

Figure 1: Schematic of Analytical 8DOF System

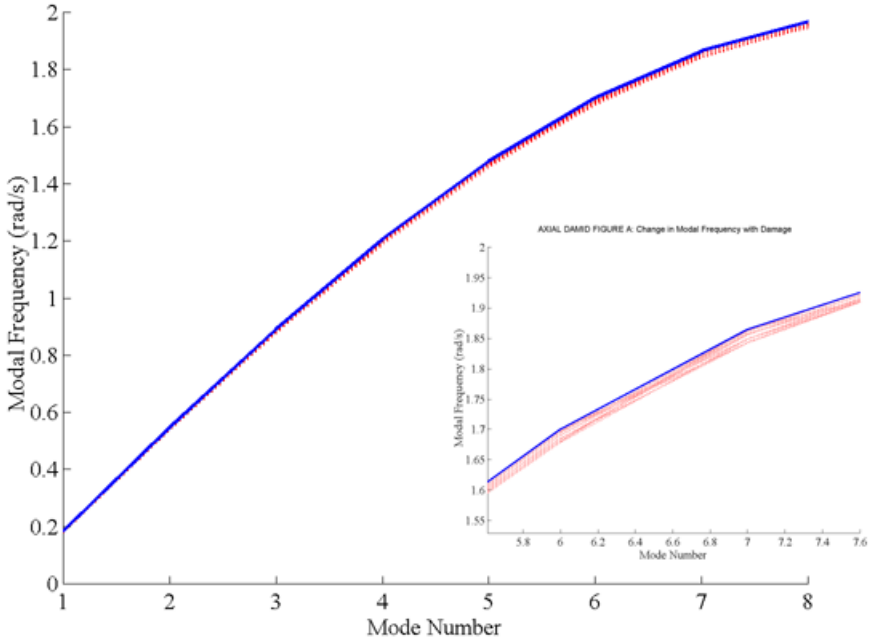

Figure 2: Change in Modal Frequency with 10% Damage

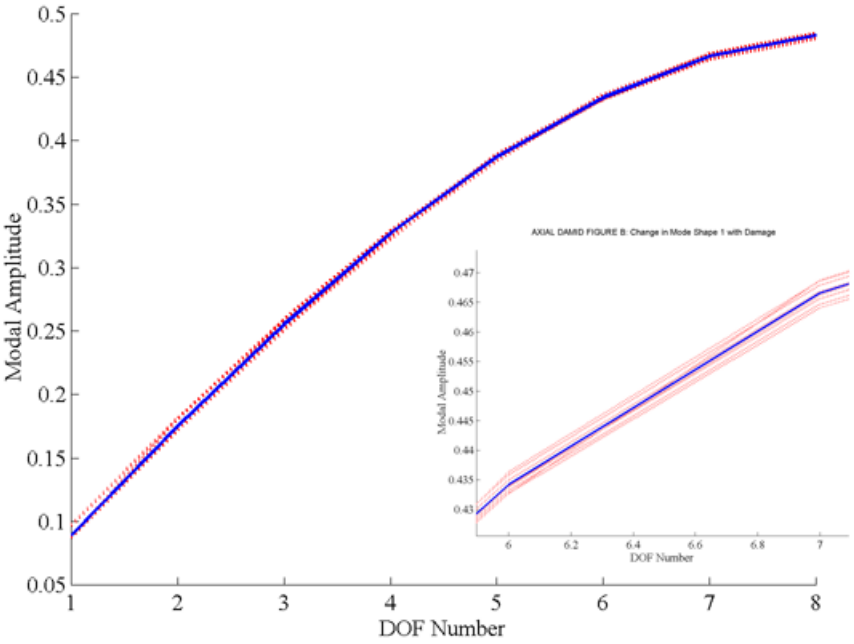

Figure 3: Change in First Mode Shape with 10% Damage

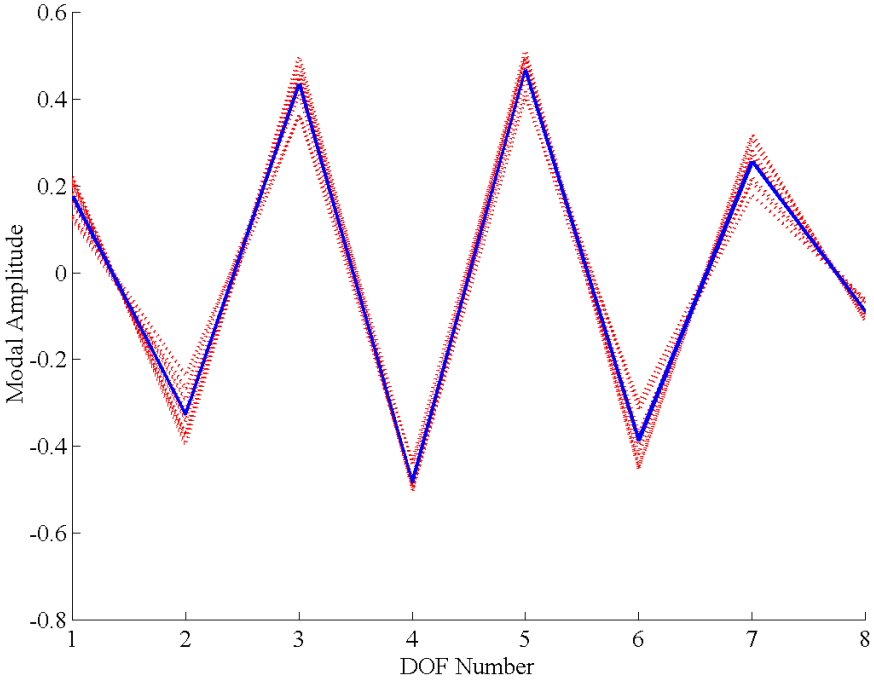

Figure 4: Change in Eighth Mode Shape with 10% Damage

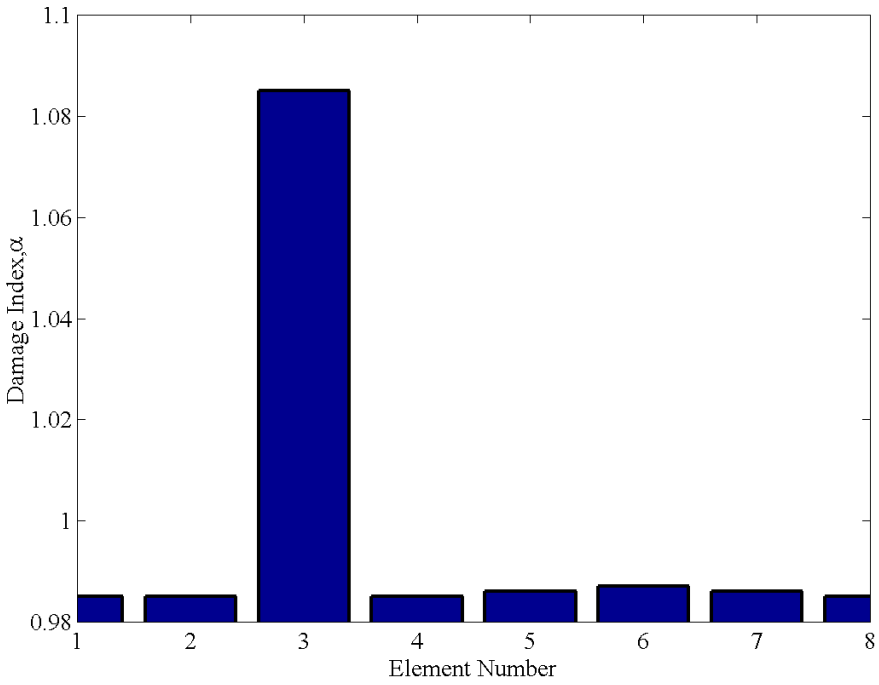

Figure 5: Damage Index Results for Simulated 8DOF System – 10% Damage in Element 3

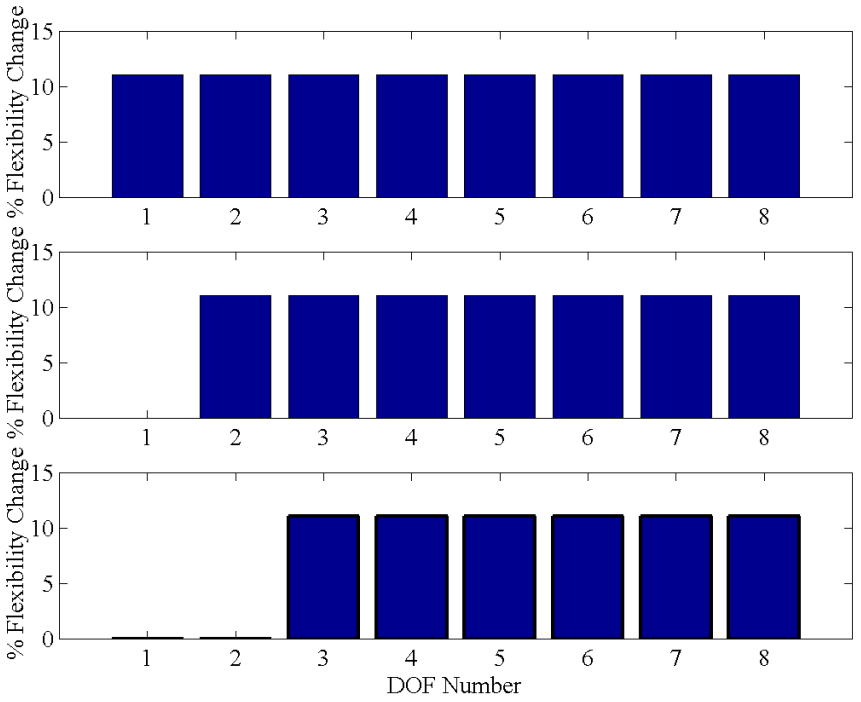

Figure 6: Change in Flexibility for 10% Damage in:
(Top) Element 1; (Middle) Element 2; (Bottom) Element 3

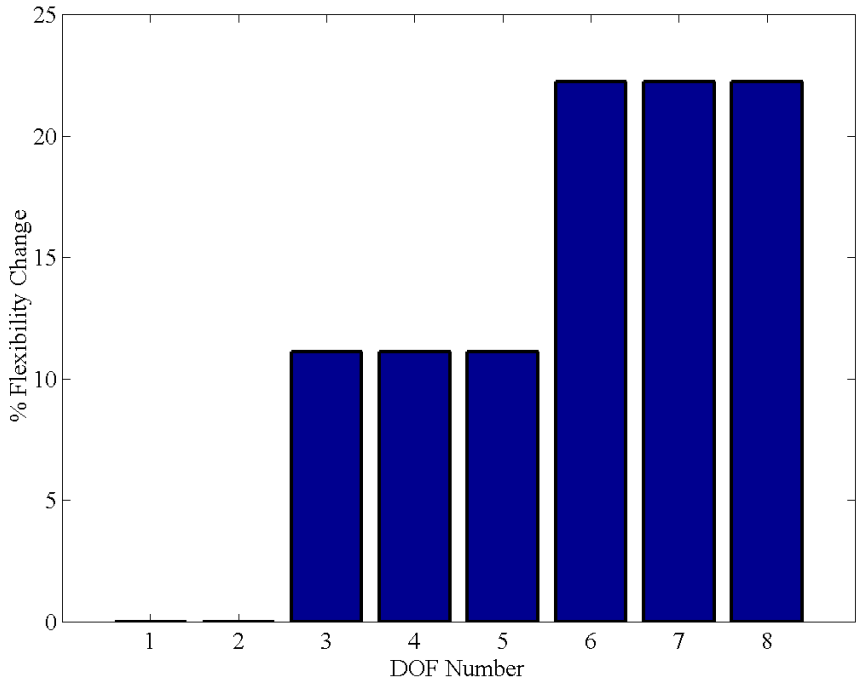

Figure 7: Change in Flexibility for Simultaneous Damage at Elements 3 and 6

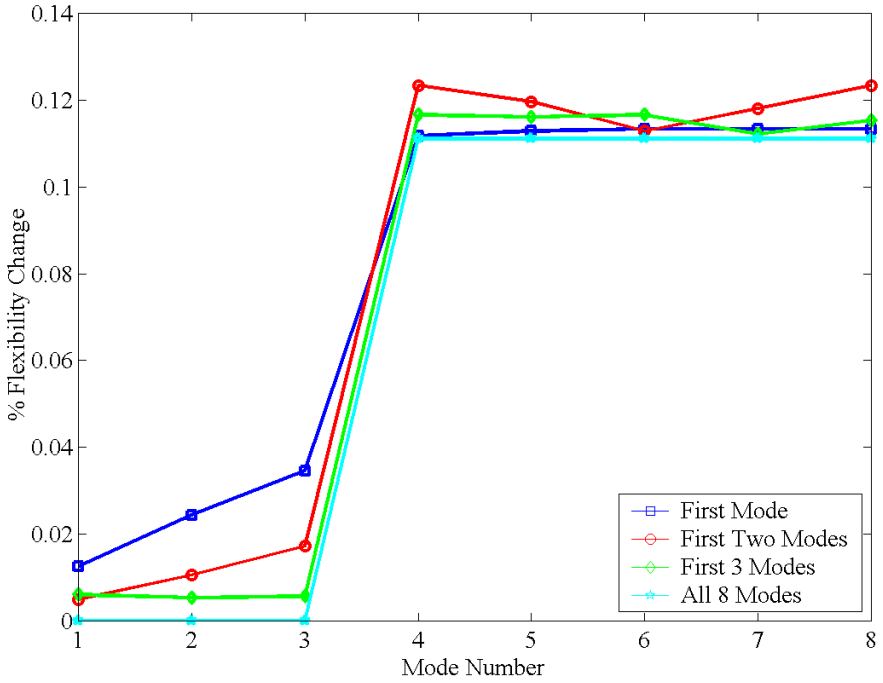

Figure 8: Influence of Number of Modes on Detection of Damage in Element 4

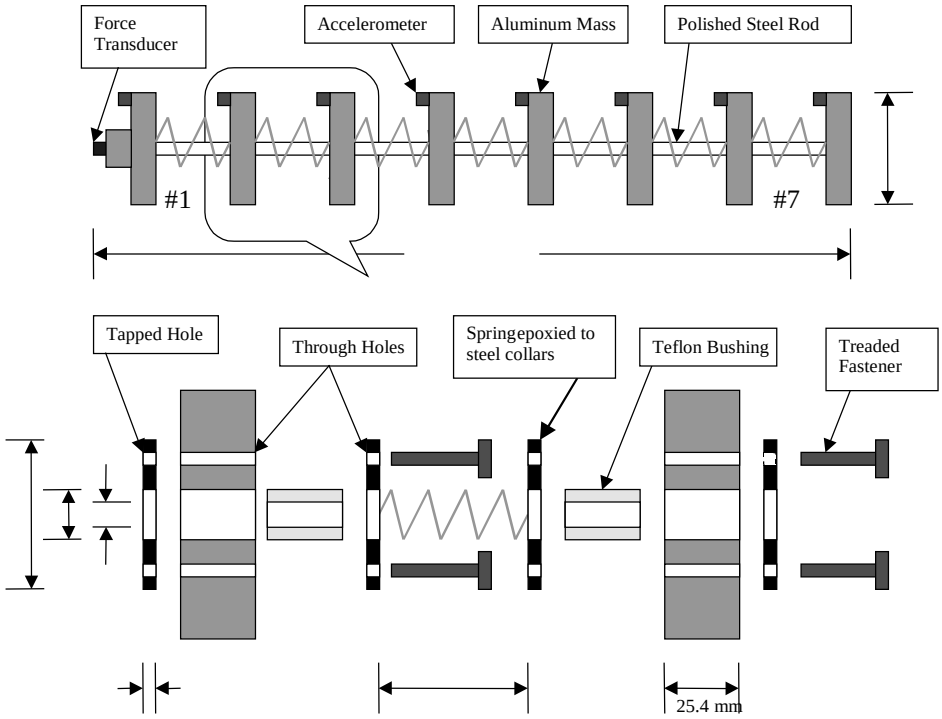

Figure 9: Schematic of Experimental 8DOF System

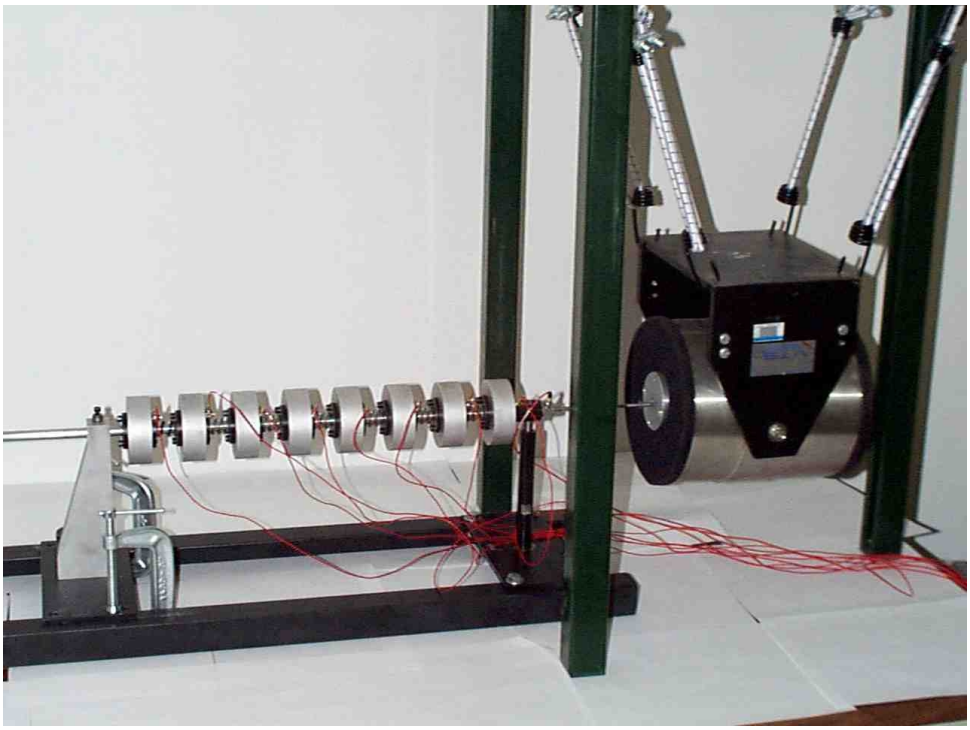

Figure 10: Experimental 8DOF System with Excitation Shaker Attached

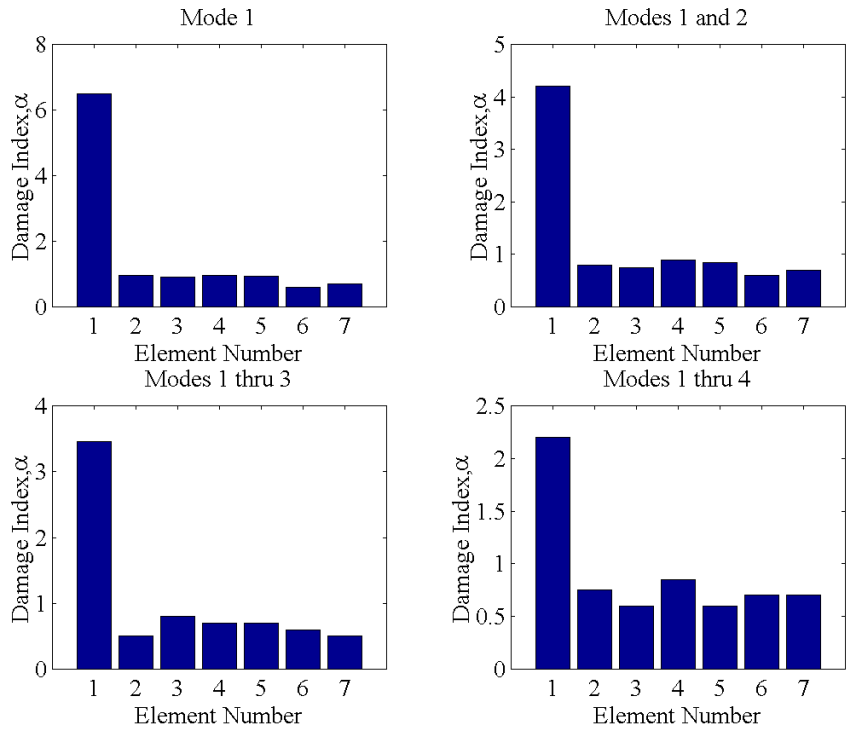

Figure 11: Damage Index Results for Experimental 8DOF System – 24% Damage in Element 1

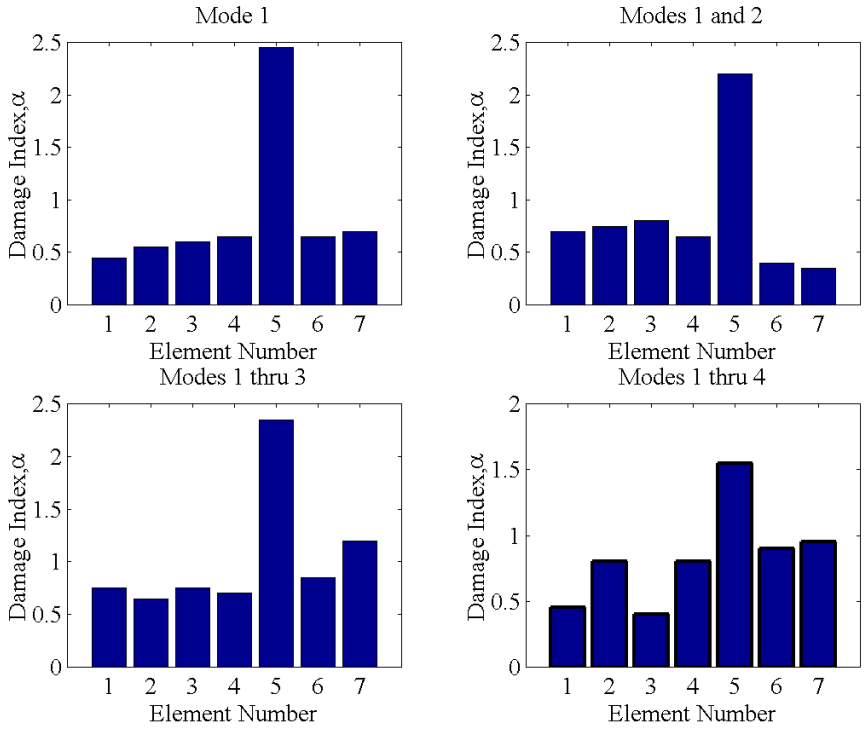

Figure 12: Damage Index Results for Experimental 8DOF System – 24% Damage in Element 5

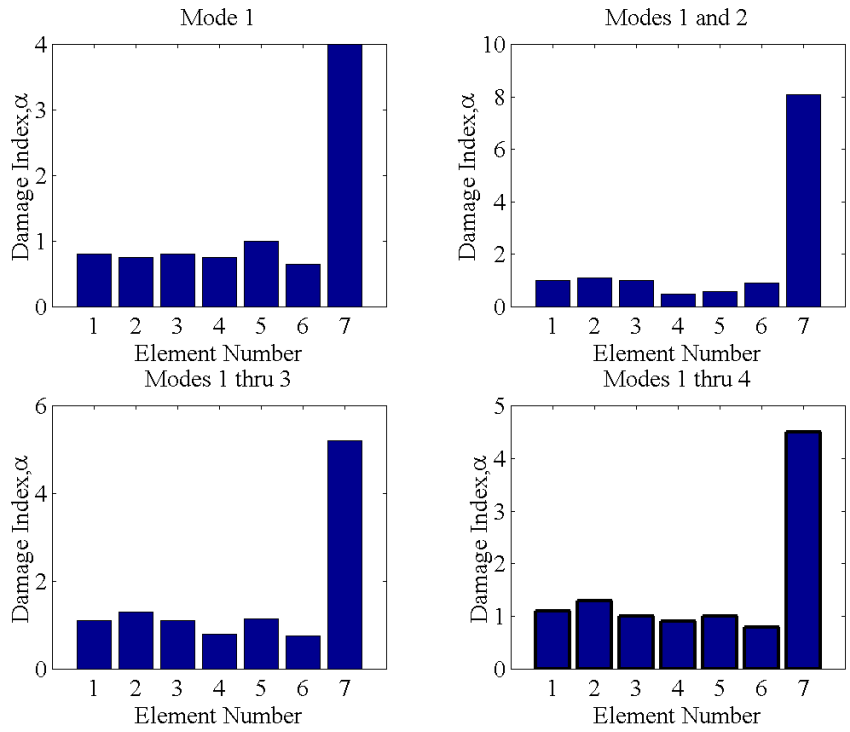

Figure 13: Damage Index Results for Experimental 8DOF System – 24% Damage in Element 7

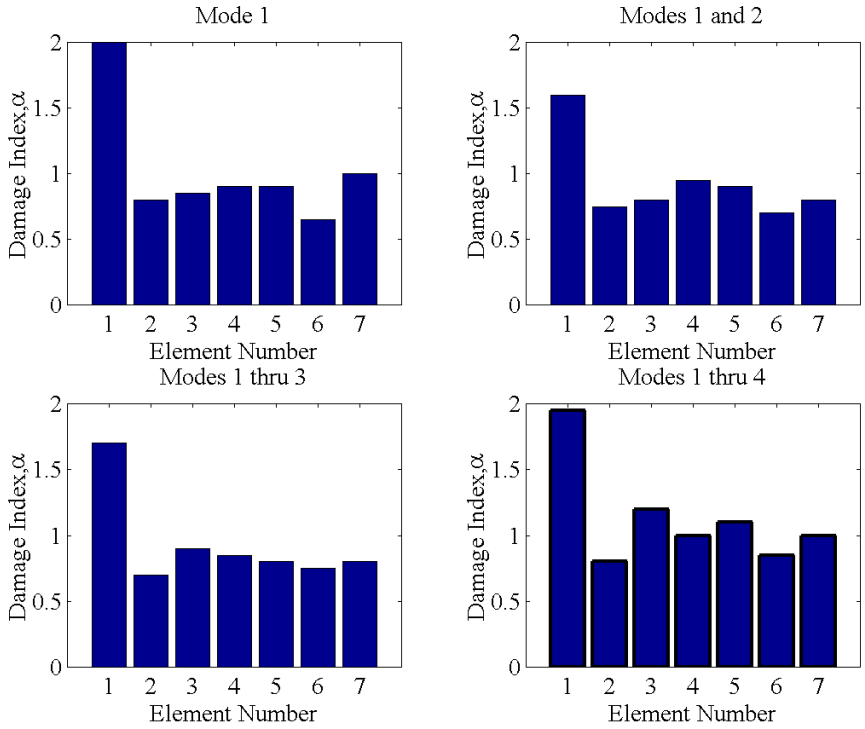

Figure 14: Damage Index Results for Experimental 8DOF System – 7% Damage in Element 1

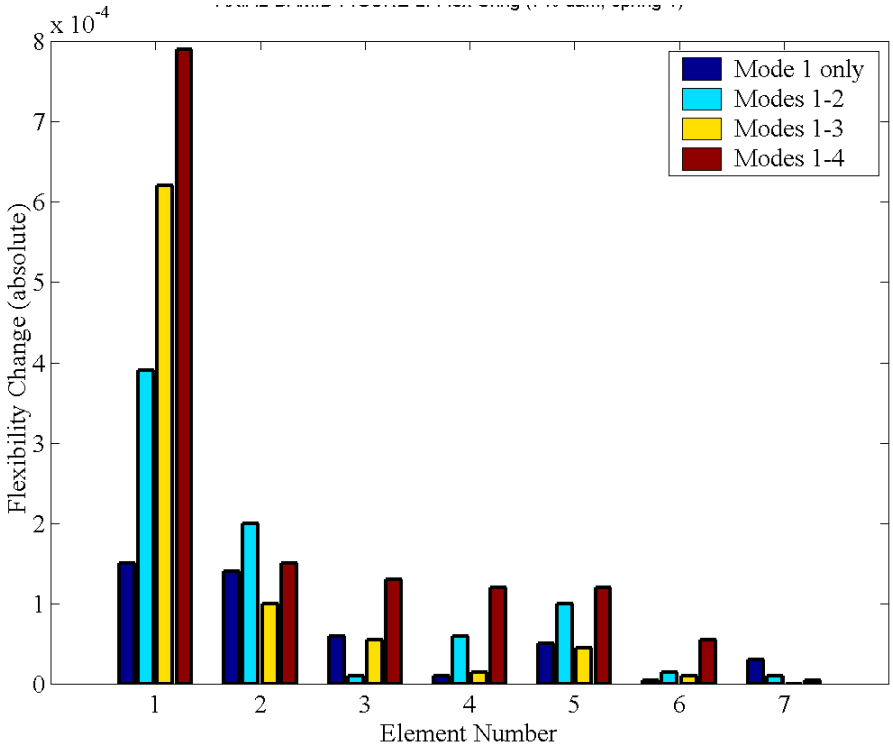

Figure 15: Flexibility Change Results for Experimental 8DOF System – 7% Damage in Element 1

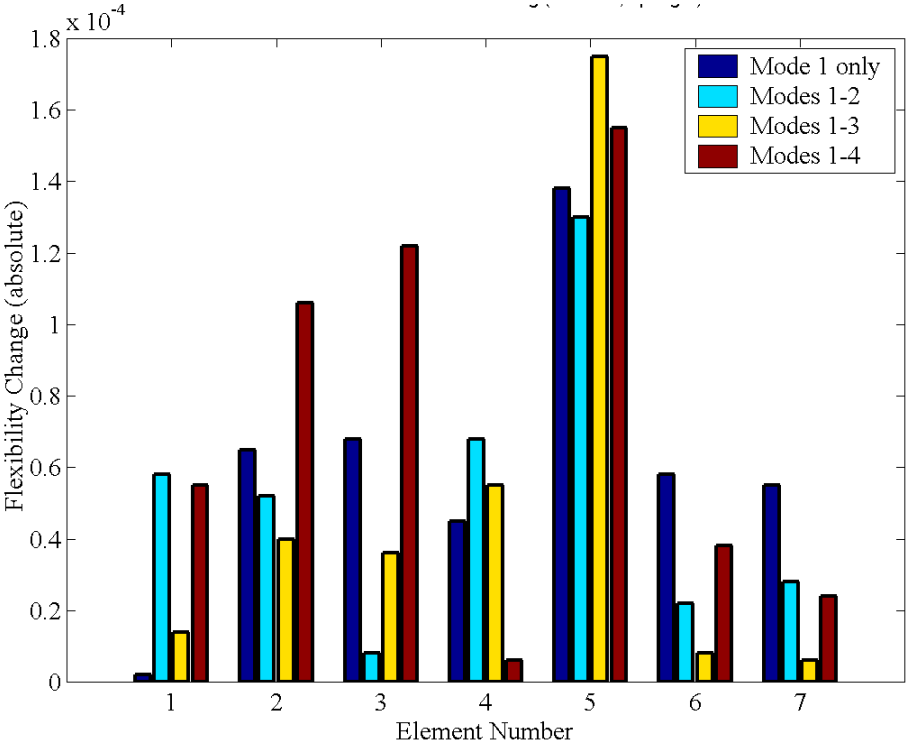

Figure 16: Flexibility Change Results for Experimental 8DOF System – 7% Damage in Element 5